The Geometric Sensitivity Analysis of Electrostatic Field for Microelectromechanical System Simulation

by

Junfeng Wang

Submitted to the Department of Electrical Engineering and Computer Science
in partial fulfillment of the requirements for the degree of

Master of Science in Electrical Engineering and Computer Science

at the

MASSACHUSETTS INSTITUTE OF TECHNOLOGY

June 1997

© Massachusetts Institute of Technology 1997. All rights reserved.

Author .....
Department of Electrical Engineering and Computer Science
May 15, 1997

Certified by .....
Jacob White
Associate Professor
Thesis Supervisor

Accepted by .....
Arthur C. Smith
Chairman, Departmental Committee on Graduate Students

MASSACHUSETTS INSTITUTE OF TECHNOLOGY

JUL 24 1997

Eng

The Geometric Sensitivity Analysis of Electrostatic Field for Microelectromechanical System Simulation

by

Junfeng Wang

Submitted to the Department of Electrical Engineering and Computer Science
on May 15, 1997, in partial fulfillment of the
requirements for the degree of
Master of Science in Electrical Engineering and Computer Science

Abstract

In this paper, a formula is derived which relates the electrostatic geometric sensitivity of the potential generated by a triangular panel charged with uniform source distribution to the potential of a linear dipole distribution on the panel. Closed form analytic formula for the potential generated by this linear dipole distribution is also derived for fast computation. Then the fast algorithm for electrostatic geometric sensitivity computation is developed by combining the linear dipole formula with the Precorrected FFT method. The fast algorithm is applied to the acceleration of the coupled algorithm of electromechanical system and to the fast computation of the geometric sensitivity of the capacitance for conductors with 3-D structure.

Thesis Supervisor: Jacob White
Title: Associate Professor

Acknowledgments

I would like to thank a number of people whose help and contributions made this work possible. My advisor Jacob White gave me strong advice throughout the research with his vision of both theory and applications. Dr. Aluru gave me important guidance in understanding both the coupled algorithm of electromechanical system and FFTCAP. Joel Phillips helped me enormously in understanding and applying FFTCAP as well as in providing tips of how to use FASTCAP. Vevik also gave me very useful tips on how to read the FFTCAP code. Mike Chou helped me a lot in the orientation in the research of the group and in numerous technical aspects. I am also very grateful to Dr. Keith Nabors for his powerful package of FASTCAP.

Contents

List of Figures

List of Tables

Chapter 1

Introduction

Fast algorithms based on Multipole- and Precorrected-FFT- accelerated boundary-element method have been commonly used to compute electrostatic forces and capacitances in complicated 3-D geometries [3, 5]. However, in applications such as solving the coupled electromechanical equations and propagating process sensitivities [1, 2], it is also necessary to compute the geometric sensitivities of the electrostatic forces or capacitances. In both cases, the problem is actually to calculate the geometric sensitivity of the electrostatic potential accurately and fast.

Because in these applications, standard piecewise constant collocation schemes are used in the discretization, the basic problem for geometric sensitivity analysis is to compute the sensitivity of the potential generated by a panel charged with uniform distributed source when the vertices are perturbed. For this problem, a formula has been derived which relates the geometric sensitivity of the potential to the potential generated by the panel with the charge of linear dipole distributions. This result can be combined with the fast potential-computing algorithm, the Precorrected FFT method [5], to develop a fast algorithm for electrostatic geometric sensitivity computation.

The steps taken from the analysis of the electrostatic geometric sensitivity for the single- panel case toward the applications mentioned in the first paragraph can be

summarized as:

1. Derive the formula for the electrostatic geometric sensitivity of a single panel with uniform source distribution.

2. Develop the fast algorithm for electrostatic geometric sensitivity computation by the combination of the formula for single panel with the Precorrected FFT method.

3. Application of the fast electrostatic geometric sensitivity computation algorithm to the acceleration of the coupled algorithm of the electromechanical system [1] and to the geometric sensitivity analysis of the capacitance of conductors with 3-D structure.

More detailed description of these steps are:

- Derive the formula for the electrostatic geometric sensitivity of a single panel charged with uniform source distribution. A formula has been derived which relates the geometric sensitivity of the potential generated by uniform source distribution to the potential generated by the panel with the charge of linear dipole distributions.

- Derivation of the closed form analytic formula for the potential of linear dipole distribution.

  The closed form formula could be derived through mathematical manipulation to turn the 2-D integration into 1-D integration and analytic form finally. The accurate and closed form analytic formula is very important in building a fast algorithm. Numerical integration will be more computationally expensive, particularly if high accuracy is required.

- Fast algorithm for electrostatic geometric sensitivity computation

A fast algorithm for electrostatic geometric sensitivity computation can be developed through the combination of the singel-panel electrostatic geometric sensitivity formula with the Precorrected FFT method.

The Precorrected FFT method is a general fast algorithm for computing the potential of 3-D structures discretized into charged panels. In this method, a 3-D uniform grid is set up, and the original charge of every panel is projected onto to the nearby grids for approximate representation of the electrical field far away from the panel. Then the potential at the grids in the whole space due to the grid charges is calculated by the FFT method, utilizing the fact that the grid is uniform so that the potential at one grid due to another is determined just by their relative position. After the grid potential is computed, the potential at the required evaluation points can be determined by backward projection from the nearby grid. However, precorrection is necessary, because the grid representation of the original potential is not accurate if the evaluation point is near the original charge. In this case, the potential is calculated directly, and the contribution due to the grid method has to be subtracted.

The implementation of Precorrected FFT in FFTCAP has two stages, a setup stage and a evaluation stage. In the setup stage, the forward projection coefficients for unit charge of the panels are evaluated and stored. Backward projection coefficients and the direct interaction coefficients are also computed and stored in the setup stage. In the evaluation stage, the forward projection coefficients are multiplied with the real charge to get the grid representation for FFT computation. The overhead of setup is large, but the evaluation stage is very fast. This is exactly the reason of the high efficiency of FFTCAP. In FFTCAP, Precorrected FFT is used to evaluate the potential due to the charged panels at fixed position with different sets of uniform source distributions. There is only one setup stage for estimation of the projection coefficients, while the evaluation stage of the algorithm is used many times.

The combination of the dipole formula through Precorrected FFT method will result in the fast algorithm of geometric sensitivity of the electrostatic field. The algorithm will also have two stages, a slow setup stage and a fast evaluation stage. In the setup stage, the coefficients of the derivatives of the electrostatic potential with respect to all directions of the displacement of the vertices of the panels are estimated and stored as well as the backward projection and direct interaction coefficients. Precorrection will also be done to the forward projection coefficients before the evaluation stage. The procedure is quite similar to the potential evaluation in FFTCAP [5], except that the charge to be projected onto the grid is a dipole distribution, not the source distribution. In the evaluation stage, the fast algorithm generates the potential change vector, $\frac{\partial P(u)}{\partial u}\hat{u}$, for any given displacement vector $\hat{u}$.

For the same reason why Precorrected FFT method of potential evaluation is fast in FFTCAP, this algorithm of geometric sensitivity will be much more efficient than a finite-difference scheme if the geometric sensitivity of the system at one position must be computed for many displacement vectors. A finite-difference scheme is slow because a new setup for potential estimation is necessary for each new displacement vector to evaluate the potential at the new position. For the fast algorithm of the electrostatic geometric sensitivity computation, however, only one setup is necessary for that position of the electrostatic system.

- Applications of the fast electrostatic geometric sensitivity computation algorithm

  1. Application of the fast electrostatic geometric sensitivity computation algorithm to the acceleration of the coupled algorithm of electromechanical system.

     To solve the coupled equations of electromechanical system, a Newton

method is used in [1]. Because GMRES is used in every Newton iteration, there are numerous evaluations of $(\frac{\partial P(u)}{\partial u}q(u))\hat{u}$, the product of Jacobian Matrix and a perturbation vector, for a given u but many different $\hat{u}$'s. It is clear that this is just the case when the fast algorithm of the electrostatic geometric sensitivity computation is faster than finite difference method. The current method in [1] is the approximation of the matrix-vector product by a finite difference scheme of evaluating $\frac{1}{\epsilon}(P(u+\epsilon\hat{u})q(u)-P(u)q(u))$, where ϵ is small. The fast algorithm of the electrostatic geometric sensitivity computation will accelerate the coupled algorithm by replacing the finite difference scheme.

2. Application of the fast electrostatic geometric sensitivity computation algorithm to the geometric sensitivity analysis of capacitance.

   The capacitance of a electrostatic system with position specified by the vertex position vector u can be determined by solving $P(u)q = \bar{P}$ given a vector of potentials, $\bar{P}$, and then summing entries of the charge vector q [3]. The geometric sensitivity of capacitance can be determined by the summing over the charge sensitivity $\frac{\partial q}{\partial u}\hat{u}$, which can be resolved by solving $P(u)\frac{\partial q}{\partial u}\hat{u} = -\frac{\partial P(u)}{\partial u}\hat{u}q$. After the right hand side of the equation is computed by the fast algorithm for electrostatic geometric sensitivity computation, the further calculation of $\frac{\partial q}{\partial u}\hat{u}$ is no more than the solving of a system of linear equations. This approach of sensitivity computation is faster than the finite difference method if the sensitivity along many different directions of perturbation must be computed at a fixed position of the system. Further acceleration can be achieved through adjoint method, which will be addressed later.

Chapter 2

One-panel electrostatic geometric sensitivity analysis in the standard piecewise constant collocation schemes

2.1 Problem formulation of one-panel electrostatic geometric sensitivity analysis in the standard piecewise constant collocation schemes

In standard piecewise-constant collocation schemes which are used to solve integral formulations of electrostatic problems, the fundamental problem of electrostatic geometric sensitivity is that of a one-panel case. For the one-panel case, the task is to derive the formula for the sensitivity of the potential generated by a panel with a uniform charge distribution when the panel vertices are perturbed. In this thesis, the sensitivity to the perturbation of one vertex of a triangular panel is analyzed first because it is the most basic case. An illustration of this case is in figure 2-1.

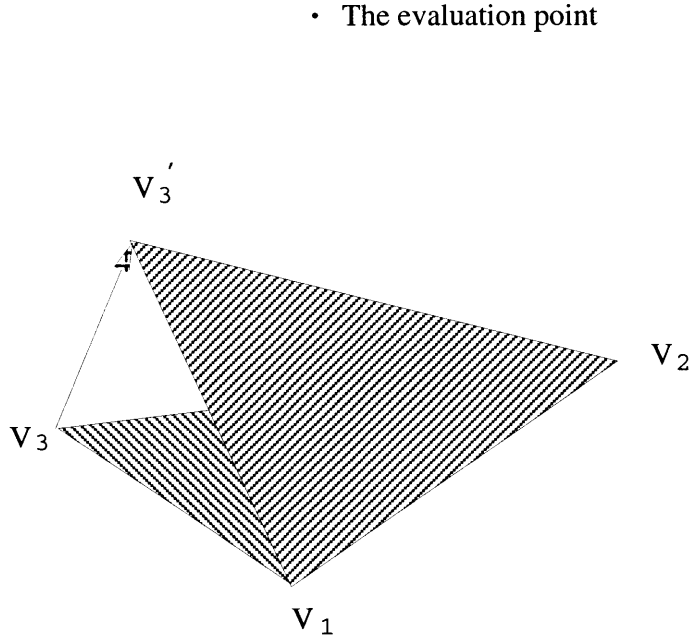

Figure 2-1: The typical case for electrostatic geometric sensitivity analysis

In the perturbation, two assumptions in the collocation scheme should be satisfied:

1. The the charge on the panel is uniformly distributed regardless of the perturbation.

2. The net charge on the panel is unchanged at any position of the perturbation.

The perturbation can be parameterized as in the figure 2-2.

In the figure 2-2, unit length vector $\vec{d}$ is the direction of the displacement of the perturbed vertex, and t is the distance of the perturbation.

Then the charge density, domain of the panel and the potential at an evaluation point are all functions of t, denoted as $\rho(t)$, $S(t)$ and $\bar{P}(t)$, respectively.

The electrostatic geometric sensitivity is defined to be $\frac{d\bar{P}(t)}{d\ t}|_{t=0}$, the sensitivity of $\bar{P}(t)$ to the perturbation along $\vec{d}$.

The evaluation point could be off the panel or on the panel. If the evaluation point is off the panel, it is fixed when the vertex is perturbed; If the evaluation point

• The evaluation point

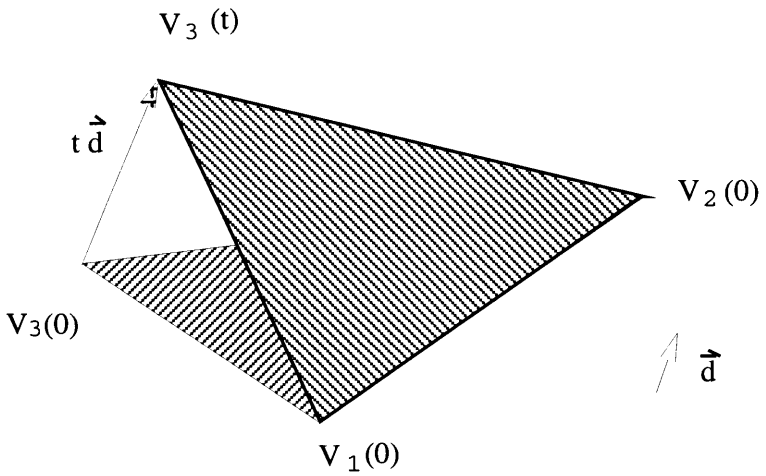

Figure 2-2: The parameterization of the perturbation

is on the panel, it moves along with the perturbation of the vertex. In most of the applications, the on-panel evaluation point is actually the centroid of the triangle. In the following sections, the off-panel formula is derived first whereas the on-panel case discussed later because of its added complexity.

2.2 Electrostatic geometric sensitivity for off-panel case

Electrostatic geometric sensitivity for off-panel case is just the potential due to the charge of a linear dipole distribution on the panel. The derivation of the formula is based on the mapping of points both intuitively and mathematically:

2.2.1 Mapping of the points

• The evaluation point

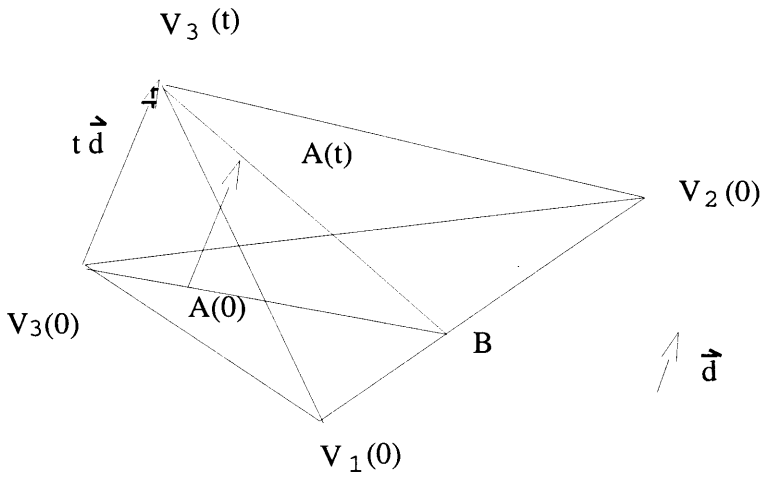

Figure 2-3: The mapping of the points

A one-to-one mapping of the points on the original panel to those on the new panel is shown in the figure 2-3.

From the figure 2-3, at any fixed t, an arbitrary point $A(0)$ on the initial panel can be mapped from the original position to its new position A(t) on the new panel with the displacement $\epsilon\vec{d}$, where $\epsilon = \frac{|A(0)B|}{|V_3(0)B|}$.

Exploration of the area changing ratio of the mapping by the algebraic perspective

Another mapping defined in an algebraic way is introduced here and can be shown to be the the same as the former one.

The algebraic definition of the mapping is based on the parameterization of the triangle:

$$\vec{a} = c_1\vec{v}_1 + c_2\vec{v}_2 + c_3\vec{v}_3 \tag{2.1}$$

where $\vec{a}$ is the coordinates of an arbitrary point on the original triangle, $\vec{v_1}$, $\vec{v_2}$ and $\vec{v_3}$ are the coordinates of the vertices. The coefficients of the parameterization are c_1, c_2 and c_3.

Under the parameterization, the mapping can be defined as

$$T_t: \quad \vec{a} = c_1\vec{v}_1 + c_2\vec{v}_2 + c_3\vec{v}_3 \rightarrow \vec{a}(t) = c_1\vec{v}_1 + c_2\vec{v}_2 + c_3\vec{v}_3(t) \tag{2.2}$$

From the definition, the direction of the displacement of every point on the triangle is parallel to that of V_3, $\vec{d}$.

It is clear the two mapping shown above are exactly the same, because they have the same effect on every point of the original panel. In both mapping, every point on the original panel undergoes the displacement parallel to $\vec{d}$ to the new position on the new panel.

With the algebraic perspective of the mapping, it is clear that the change of area due to the mapping around any point is exactly the same, because the transformation is linear.

2.2.2 The mapping of the charge

Figure 2-4 is an illustration of the mapping of the charge, which is simply mapping the charge carried by any point to the correspondent point on the new panel. The significance of the mapping of the charge is that the two assumptions about the charge are automatically satisfied:

1. The the charge on the panel is uniformly-distributed source charge

   Consider the change of charge density around an arbitrary point $A(0)$ with a small disk around it, $ds(0)$. After the mapping, the point and the disk becomes $A(t)$ and $ds(t)$. The charge density around $A(0)$ is the original charge density over the whole panel, $\rho(0)$. Assume the charge density around $A(t)$ is $\rho(t)$.

- The evaluation point

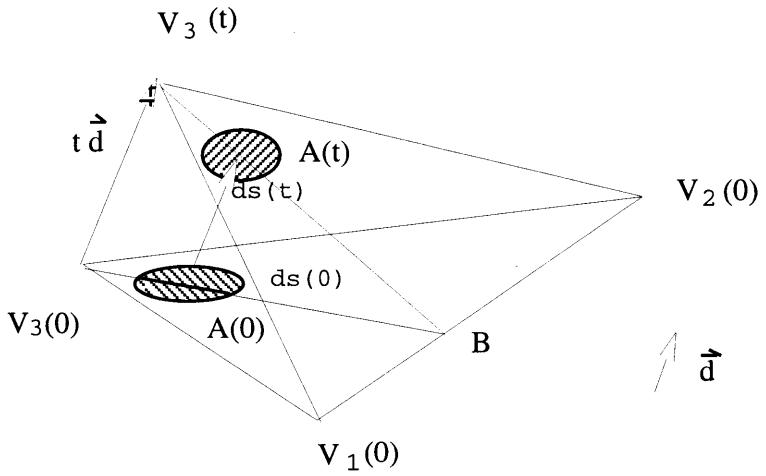

Figure 2-4: The mapping of the charge

From the mapping of the charge, the net charge over the disk $ds(0)$ is the same as that over the new disk $ds(t)$, so the following equation holds:

$$\rho(0)ds(0) = \rho(t)ds(t) \tag{2.3}$$

Since the ratio of the area of $ds(t)$ over that of $ds(0)$ is constant over the whole panel, just denote the ratio by λ. Then:

$$\rho(t) = \frac{\rho(0)}{\lambda} \tag{2.4}$$

Both $\rho(0)$ and λ are constant over the panel, then $\rho(t)$ is also constant over the whole panel. Therefore, the mapping of the charge results in uniformly-distributed source charge.

2. The net charge on the panel is unchanged.

This is true because all the charge on the original panel is mapped onto the new panel.

Since the mapping obeys the assumptions of charge during perturbation, it can be used to compute the potential sensitivity.

2.2.3 The linear dipole formula

The potential generated by the panel without perturbation is:

$$\bar{P}(0) = \iint_{S(0)} \frac{1}{r(0)} \rho(0) ds(0) \tag{2.5}$$

With the mapping in mind, the potential at t is just the integration of the potential of mapped charge of the points throughout the whole panel:

$$\bar{P}(t) = \iint_{S(t)} \frac{1}{r(t)} \rho(t) ds(t) \tag{2.6}$$

where the integrand is evaluated at an arbitrary point $A(t)$ on the panel at t, with $\vec{r}(t)$ as the vector from $A(t)$ to the evaluation point. All the terms of the integrand of equation 2.6 are related correspondingly to those of equation 2.5 by the mapping through point.

With equation 2.3, equation 2.6 can be simplified so that the integration is done on the original triangular domain $S(0)$:

$$\bar{P}(t) = \iint_{S(0)} \frac{1}{r(t)} \rho(0) ds(0) \tag{2.7}$$

Then the geometric sensitivity of $\bar{P}(t)$ is:

$$\frac{d\bar{P}(t)}{d\ t}|_{t=0} = \iint_{S(0)} \frac{\partial(\frac{1}{r(t)})}{\partial t}|_{t=0}\ \rho(0) ds(0) \tag{2.8}$$

The term $\frac{\partial(\frac{1}{r(t)})}{\partial t}|_{t=0}$ can be related to a dipole, which is made clear by the figure 2-5.

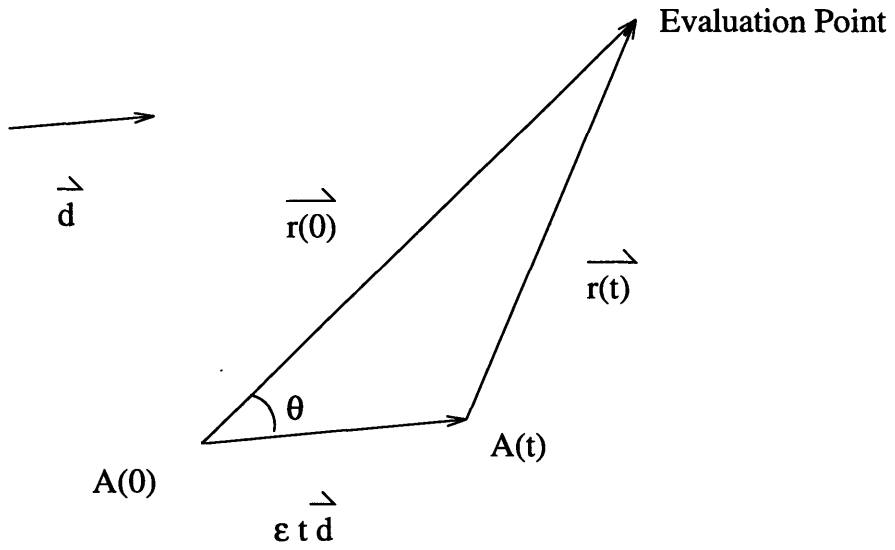

Figure 2-5: Dipole nature of the potential change

From the figure 2-5, it is clear that $\frac{\partial(\frac{1}{r(t)})}{\partial t}|_{t=0}$ is just the derivative of the potential at the evaluation point generated by a monopole due to its displacement from $A(0)$ to $A(t)$ in the direction of $\vec{d}$ and the distance of ϵt. In the figure, θ is the angle between the line from $A(0)$ to the evaluation point and the line from $A(t)$ to the evaluation point.

Then it can be written as the potential generated by a dipole at $A(0)$ with $\vec{d}$ and ϵ as its direction and intensity:

$$\frac{\partial(\frac{1}{r(t)})}{\partial t} = \frac{\epsilon \cos\theta}{r(0)^2} \tag{2.9}$$

With this result, the sensitivity of the potential generated by the panel is just the potential generated by a linear dipole distribution on the panel:

$$\frac{d\bar{P}(t)}{dt}|_{t=0} = \iint_{S(0)} \frac{\epsilon \cos\theta}{r(0)^2} \rho(0) ds(0) \tag{2.10}$$

2.3 Electrostatic geometric sensitivity for on-panel evaluation point

For the on-panel case in the collocation scheme, the evaluation point is the center of the triangle. Because the evaluation point is moving along with the vertex in the perturbation, the potential change can be decomposed into two parts, one from the contribution of the displacement of the vertex with a fixed center, another from the displacement of the center with a fixed vertex.

Meanwhile, the displacement can always be decomposed into a normal component and a tangential component. The sensitivity along the tangential direction will be shown to be the potential of a linear dipole distribution plus the contribution from the displacement of the center due to the electrostatic field. The sensitivity along the normal direction is zero because the contribution from the two parts will cancel.

2.3.1 The contribution to the sensitivity from the vertex

In considering the contribution only from the vertex, the center of the triangle is held fixed at the original place while the vertex is perturbed. Still, equation 2.7 holds although the center of the panel is a singular point of the integrand. But the linear dipole formula has to be modified because there will be differentiation of the integration around the singularity point which needs special care. Around the singular point, integration and differentiation is no longer guaranteed to be commutative. However, a cut can be made into the domain of integration of equation 2.7 to make the change of order valid except around the singular point.

In the figure 2-6, $C(0)$ is the original position of the center, $C(t)$ is the image of $C(0)$ by the mapping at t. $\bar{S}(D,0)$ is a disk around $C(0)$ with D as its radius, and $\bar{S}(D,t)$ as its image of the mapping.

Since the order exchange of the integration with differentiation is still justified in the domain $S(0) - \bar{S}(D,0)$, the sensitivity of the potential is:

• The evaluation point

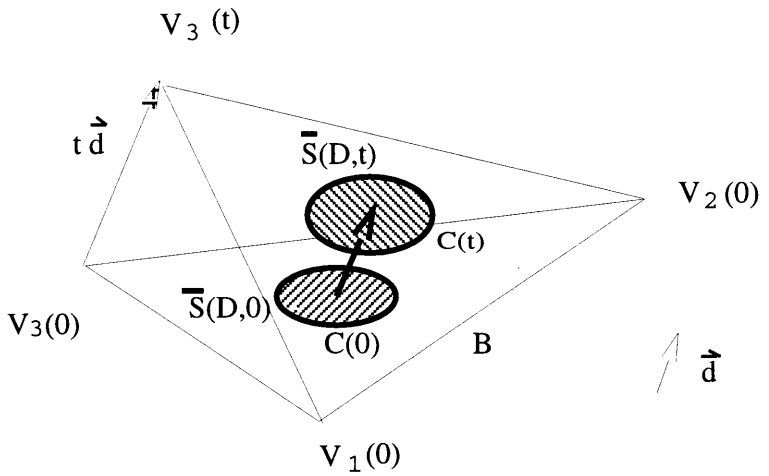

Figure 2-6: Exclusion of the singular point of the integration region

$$\frac{d\bar{P}(t)}{dt} = \iint_{S(0)-\bar{S}(D,0)} \frac{\epsilon \cos\theta}{r(0)^2}\rho(0)ds(0) + \frac{d}{dt}\left(\iint_{\bar{S}(D,0)} \frac{1}{r(t)}\ \rho(0)d\bar{s}(D,0)\right)|_{t=0} \quad (2.11)$$

Let D go to 0, then:

$$\frac{d\bar{P}(t)}{dt} = \iint_{S(0)} \frac{\epsilon \cos\theta}{r(0)^2}\rho(0)ds(0) + k(\vec{d}\,) \quad (2.12)$$

where

$$k(\vec{d}\,) = \lim_{D\to 0} \frac{d}{dt}\left(\iint_{\bar{S}(D,0)} \frac{1}{r(t)}\ \rho(0)ds(D,0)\right)|_{t=0}$$

In the equations above, $k(\vec{d}\,)$ is the kernel of sensitivity around the singularity point along the perturbation direction $\vec{d}$.

It will be proved in the coming sections that $k(\vec{d}\,)$ is 0 if $\vec{d}$ is tangential to the panel, while it is $-\frac{2\pi}{3}\rho_0$ if $\vec{d}$ is along the normal direction of the panel.

Denote K_t as the kernal $k(\vec{d}\,)$ for any $\vec{d}$ tangential to the panel, and K_n as the kernal for $\vec{d}$ along the normal direction of the to panel, then:

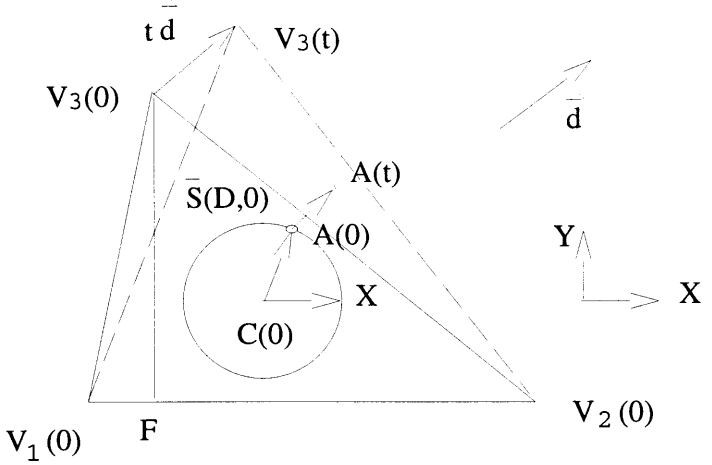

Figure 2-7: Domain for computation of tangential kernel

1. $K_t = 0$ for tangential perturbation,

2. $K_n = -\frac{2\pi}{3}\rho_0$ for normal perturbation.

Kernel of the tangential direction

It is going to be shown that the tangential kernel is zero by decomposing it into several terms where every term is zero.

At certain value of D, consider $\frac{d}{dt}(\iint_{\bar{S}(D,0)} \frac{1}{r(t)}\ \rho(0)d\bar{s}(D,0))|_{t=0}$.

In the figure 2-7, $\bar{S}(D,0)$ is the domain of computation for the tangential kernel, AF is the height on $V_2(0)V_3(0)$, with length H, A is an arbitrary point on the boundary of $\bar{S}(D,0)$, and X axis is in the same direction as side $V_2(0)V_3(0)$. After the perturbation, the disk is $\bar{S}(D,t)$.

The potential change due to the perturbation of $\bar{S}(D,0)$ at t is:

$$\delta\bar{P}(D,t) = \iint_{\bar{S}(D,t)} \frac{\rho(t)}{r(t)} d\bar{s}(D,t) - \iint_{\bar{S}(D,0)} \frac{\rho(0)}{r(0)} d\bar{s}(D,0) \tag{2.13}$$

The kernel is:

$$\lim_{D\to 0}\lim_{t\to 0} \frac{\delta\bar{P}(D,t)}{t}$$

For any point A on the boundary of $\bar{S}(D,0)$, the displacement is $\epsilon t\vec{d}$, where $\epsilon = \frac{D}{H}\sin\alpha + \frac{1}{3}$.

This can be interpreted that the disk has undergone two stages of perturbation, the first one is a shift from the original place by $\frac{t}{3}$ in the direction of $\vec{d}$, another is a symmetric stretch around the center after the shift.

With the insertion of the potential due to the shifted disk, which is denoted as $\bar{S}'(D,t)$, this interpretation results in the transformation of 2.13 into:

$$\delta\bar{P}(D,t) = \delta\bar{P}_1(D,t) + \delta\bar{P}_2(D,t) \tag{2.14}$$

where

$$\delta\bar{P}_1(D,t) = \iint_{\bar{S}(D,t)} \frac{\rho(t)}{r(t)} d\bar{s}(D,t) - \iint_{\bar{S}'(D,t)} \frac{\rho(0)}{r(t)} d\bar{s}'(D,t)$$

and

$$\delta\bar{P}_2(D,t) = \iint_{\bar{S}'(D,t)} \frac{\rho(0)}{r(t)} d\bar{s}'(D,t) - \iint_{\bar{S}(D,0)} \frac{\rho(0)}{r(0)} d\bar{s}(D,0)$$

The second term, $\delta\bar{P}_2(D,t)$, is the potential changed at the fixed point of C(0) due to the shift of the disk $\bar{S}(D,0)$, which is the same as the potential change due to the shift of the evaluation point from $C(0)$ in the opposite direction of $\vec{d}$ in the same distance while the disk is fixed. Therefore, sensitivity can be determined by the tangential component of the electrostatic field gradient at the center of the disk, $\nabla_{tan}\bar{P}$:

$$\lim_{t\to 0} \frac{\delta\bar{P}_2(D,t)}{t} = \frac{1}{3}\nabla_{tan}\bar{P} \bullet \vec{d}$$

The tangential component of the electrostatic gradient is zero at the center of the disk because the electrostatic field is symmetric in all tangential direction. Therefore, the contribution of the second term to the tangential kernel is zero.

The first term is the potential change due to a symmetric stretch of the shifted disk. The shift of the disk is $\frac{1}{3}t$ from the original position, and the stretch after the

shift is, for any point A on the boundary of $\bar{S}(D,0)$, the displacement after the shift is $\frac{D}{H}t\sin\alpha\ \ \vec{d}$. The maximum amount of stretch is $\frac{D}{H}t$.

General SHIFT and STRETCH need to be defined for further manipulation of the first term. Since the displacement of the boundary point is enough to define the shift or stretch for potential change, the arbitrary boundary point A shown in Figure 2-7 will be used in the definition.

A general SHIFT by u can be defined as, the shift of $\bar{S}(D,0)$ by $u\vec{d}$, and a general STRETCH can be defined by the maximum amount of stretch, v. The STRETCH by v after the SHIFT of the disk $\bar{S}(D,0)$ is that, for any point originally at A as in Figure 2-7 on the boundary of $\bar{S}(D,0)$, move it by $v\sin\alpha\vec{d}$.

Define function $g(u,v)$ as the potential at the fixed evaluation point $C(0)$ generated by the disk resulted from a STRETCH by v after a SHIFT by u of the original disk $\bar{S}(D,0)$, then it follows naturally that the first term of the potential change is:

$$\delta\bar{P}_1(D,t) = g(u(t),v(t)) - g(u(t),0)$$

where $u(t) = \frac{1}{3}t$, and $v(t) = \frac{D}{H}t$. To evaluate its contribution to the kernel, consider:

$$\lim_{t\to 0}\frac{\delta\bar{P}_1(D,t)}{t} = \frac{D}{H}\frac{\partial g}{\partial v}(0,0) \tag{2.15}$$

It will be shown in the following discussion that $\frac{\partial g}{\partial v}(0,0)$ is bounded so that $\lim_{t\to 0}\frac{\delta\bar{P}_1(D,t)}{t}$ is $O(D)$. Then it is clear that $\delta\bar{P}_1(D,t)$ has zero contribution to the tangential kernel either.

The symmetric stretch is shown in the figure 2-8:

The proof that $\frac{\partial g}{\partial v}(0,0)$ is bounded:

To compute $\frac{\partial g}{\partial v}(0,0)$, consider $g(0,v) - g(0,0)$:

$$\begin{aligned} g(0,v) - g(0,0) &= \iint_{S_s(v)}\frac{\rho(v)}{r(v)}ds_s(v) - \iint_{\bar{S}(D,0)}\frac{\rho(0)}{r(0)}d\bar{s}(D,0) \\ &= \left(\iint_{S_s(v)}\frac{\rho(v)}{r(v)}ds_s(v) - \iint_{\bar{S}(D,0)}\frac{\rho(v)}{r(0)}d\bar{s}(D,0)\right) \end{aligned}$$

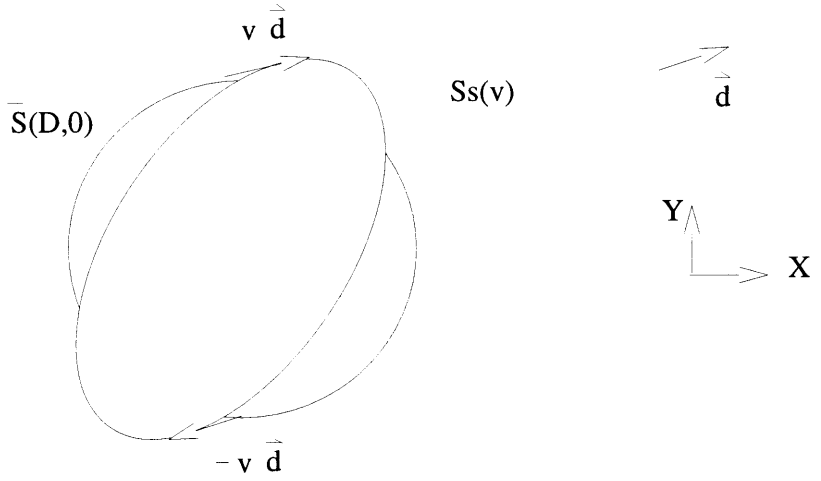

Figure 2-8: Symmetric stretch of the disk without shift

$$+\iint_{\bar{S}(D,0)} \frac{\rho(v)-\rho(0)}{r(0)} d\bar{s}(D,0)$$

The second term in the right hand side of the equation above has no contribution to the tangential kernel because its contribution to $\frac{\partial g}{\partial v}(0,0)$ is bounded:

$$\lim_{v\to 0} \frac{1}{v} \iint_{\bar{S}(D,0)} \frac{\rho(v)-\rho(0)}{r(0)} d\bar{s}(D,0) = 2\pi\rho'(0)D$$

Because the original disk and the stretched one are on the same plane, $r(v)$ and $r(0)$ are essentially the same as a term of the integrand. Then the first term of the right hand side of the equation of $g(0,v) - g(0,0)$ is the difference of integration of the same positive integrand over two overlapping domain, so it can be bounded by the integration over a domain that includes all the region not overlapped. Because the maximum perturbation of the points on the boundary of $\bar{S}(D,0)$ is v, the region not overlapped can be enclosed by a ring denoted by $Ring(v)$ which is around $C(0)$ with $D-v$ as its inner radius and $D+v$ as its outer radius. Therefore, the absolute value of the first term is bounded by:

$$\iint_{Ring(v)} \frac{\rho(v)}{r} ds = 4\rho(v)\pi v$$

And with:

$$\lim_{v\to 0}\frac{1}{v}(4\rho(v)\pi v) = 4\rho(0)\pi$$

the contribution to $\frac{\partial g}{\partial v}(0,0)$ from the first term is also bounded. So $\frac{\partial g}{\partial v}(0,0)$ is bounded, and $\delta\bar{P}_1(D,t)$ has no contribution to the tangential kernel.

From the discussion of the whole subsection, there is no nonzero contribution from any term to the tangential kernel, so it is zero.

Kernel of the normal direction

There are two major differences between normal kernel and tangential kernel:

1. The kernel, defined by

$$\lim_{D\to 0}\frac{d}{dt}(\iint_{\bar{S}(D,0)}\frac{1}{r(t)}\,\rho(0)d\bar{s}(D,0))|_{t=0}$$

   does not exist because $\iint_{\bar{S}(D,0)}\frac{1}{r(t)}\,\rho(0)d\bar{s}(D,0)$ just has one-sided derivative around $t=0$ because of the symmetry of the electrical field. In computing the normal kernel, the derivative is computed at $t=0^+$ later.

2. The one-sided normal kernel is nonzero. The value is $-\frac{2}{3}\rho(0)\pi$.

Since the derivation of the normal kernel is quite similar to that of the tangential kernel, the derivation for the normal kernel is brief, except for the part that is unique to normal kernel.

Since the kernel is defined by:

$$\lim_{D\to 0}\frac{d}{dt}(\iint_{\bar{S}(D,0)}\frac{1}{r(t)}\,\rho(0)d\bar{s}(D,0))|_{t=0^+}$$

Define $\delta\bar{P}(D,t)$ as in equation 2.13. Similar to the tangential case, insert the potential due to a shifted disk as an intermediate term in $\delta\bar{P}(D,t)$ to break it into two terms:

$$\delta\bar{P}(D,t) = \delta\bar{P}_1(D,t) + \delta\bar{P}_2(D,t)$$

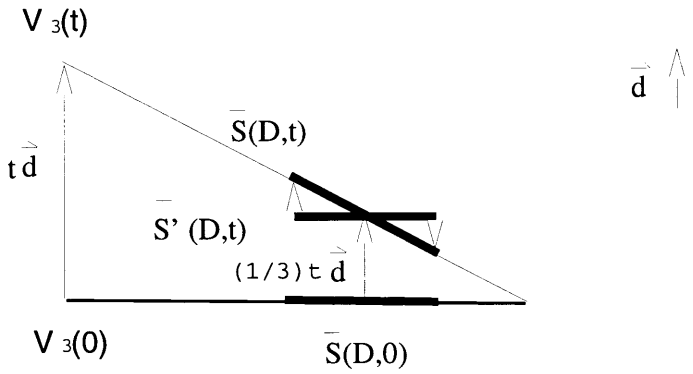

Figure 2-9: Side view of the disks for computation of normal kernel

where

$$\delta\bar{P}_1(D,t) = \iint_{\bar{S}(D,t)} \frac{\rho(t)}{r(t)} d\bar{s}(D,t) - \iint_{\bar{S}'(D,t)} \frac{\rho(0)}{r(t)} d\bar{s}'(D,t)$$

and

$$\delta\bar{P}_2(D,t) = \iint_{\bar{S}'(D,t)} \frac{\rho(0)}{r(t)} d\bar{s}'(D,t) - \iint_{\bar{S}(D,0)} \frac{\rho(0)}{r(0)} d\bar{s}(D,0)$$

The figure 2-9 is a side view of the position of the three disks.

While $\delta\bar{P}_1(D,t)$ still has zero contribution to the kernel, which will be shown later, $\delta\bar{P}_2(D,t)$ contributes:

$$\begin{aligned} \delta\bar{P}_2(D,t) &= \int_0^{2\pi}\int_0^D \frac{\rho(0)r}{\sqrt{r^2 + (\frac{t}{3})^2}} dr d\alpha - 2\pi D\rho(0) \\ &= -\frac{2\pi}{3}\rho(0)t + O(t^2) \end{aligned}$$

Then:

$$\lim_{t\to 0^+} \frac{\delta\bar{P}_2(D,t)}{t} = -\frac{2\pi}{3}\rho(0)$$

To show that $\delta\bar{P}_1(D,t)$ has no contribution to the kernel as in the tangential case, define a general SHIFT and a general STRETCH perturbation of the disk the same

way as for tangential case. The only difference is that the STRETCH here also moves the disk to a different plane like a rotation.

But mathematically the same manipulation can be done in the similar way as in the tangential case.

With the same function of $g(u,v)$ as defined in the tangential case, it is clear that:

$$\delta\bar{P}_1(D,t) = g(u(t),v(t)) - g(u(t),0)$$

where $u(t) = \frac{1}{3}t$, and $v(t) = \frac{D}{H}t$. Then by one-sided differentiation:

$$\lim_{t\to 0^+} \delta\bar{P}_1(D,t) = \frac{D}{H}\frac{\partial g}{\partial v}(0,0)$$

That the $\delta\bar{P}_1(D,t)$ has zero contribution to the kernel as D goes to zero follows from the same argument as in the tangential case, which is to show that $\frac{\partial g}{\partial v}(0,0)$ is bounded.

In tangential case, the proof is based essentially on two facts:

1. The stretch does not move the disk out of the original plane.

2. The maximum amount of displacement of the boundary is small. In the tangential case, it is v, so higher order of v for maximum amount of displacement will also provide the same result.

The stretch of the normal perturbation is different from that kind of stretch, but it can be turned into that case without changing the potential to be explored. The transform is shown in the figure 2-10:

From the figure 2-10, the stretched disk $S_s(v)$ can be rotated back onto the original plane of $\bar{S}(D,0)$ to form a new disk $S_{s'}(v)$. Because the evaluation point is $C(0)$, the center of all the disks, the backward rotation does not change the potential the stretched disk generates at $C(0)$. Then the stretch and the backward rotation can be taken as one stretch of the original disk on the plane it lies on. Another important

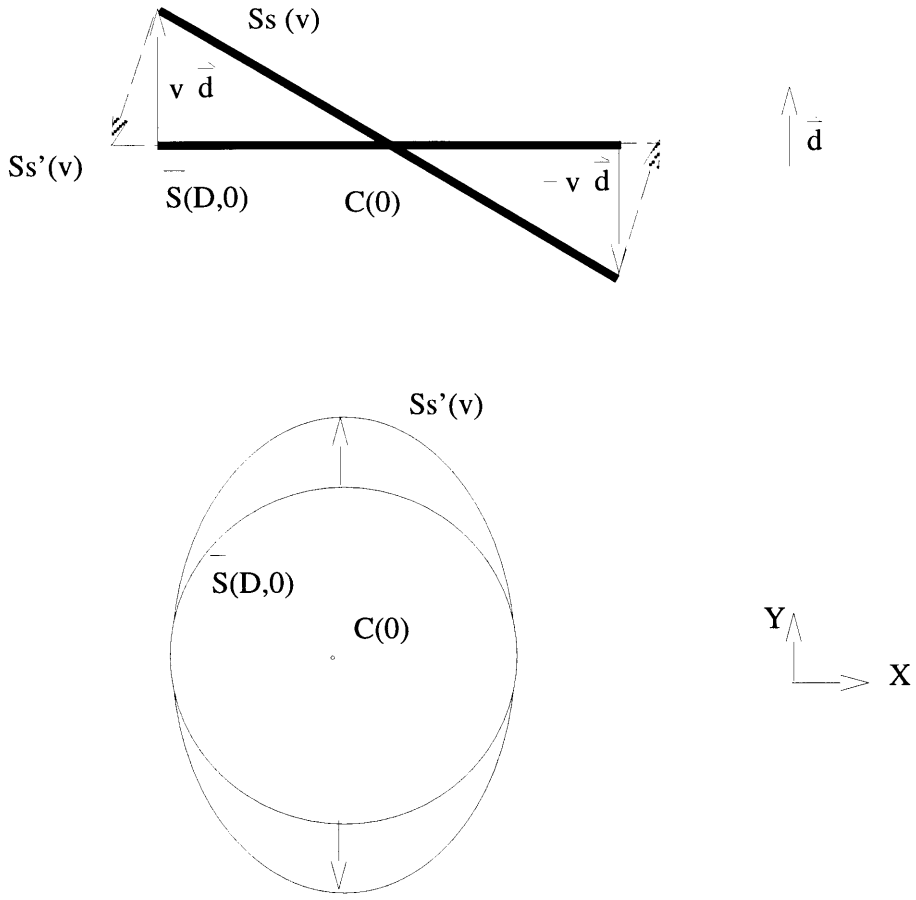

Figure 2-10: Turn the normal stretch into tangential Stretch

fact is after the new stretch, the maximum distance the point of the original disk goes is just $\sqrt{v^2 + D^2} - D$, which is $O(v^2)$.

Therefore, the new stretch satisfies both the properties necessary to conduct a similar proof as in the tangential case to show that $\frac{\partial g}{\partial v}(0,0)$ is bounded.

$$\begin{aligned} g(0,v) - g(0,0) &= \iint_{S_{s'}(v)} \frac{\rho(v)}{r(v)} ds_{s'}(v) - \iint_{\bar{S}(D,0)} \frac{\rho(0)}{r(0)} d\bar{s}(D,0) \\ &= (\iint_{S_{s'}(v)} \frac{\rho(v)}{r(v)} ds_{s'}(v) - \iint_{\bar{S}(D,0)} \frac{\rho(v)}{r(0)} d\bar{s}(D,0)) \\ &\quad + \iint_{\bar{S}(D,0)} \frac{\rho(v) - \rho(0)}{r(0)} d\bar{s}(D,0) \end{aligned}$$

The second term in the equation above has no contribution to the normal kernel because:

$$\lim_{v\to 0}\iint_{\bar{S}(D,0)}\frac{\rho(v)-\rho(0)}{r(0)}d\bar{s}(D,0)=2\pi\rho^{'}(0)D$$

The absolute value of the first term is bounded by:

$$\iint_{Ring(v)}\frac{\rho(v)}{r}ds=4\pi\rho(v)O(v^2)$$

And with:

$$\lim_{v\to 0}\frac{1}{v}(4\pi\rho(v)O(v^2))\leq 4\rho(0)\pi O(v)$$

it is clear that the contribution to $\frac{\partial g}{\partial v}(0,0)$ from the first term is also bounded. Since $\frac{\partial g}{\partial v}(0,0)$ is bounded, $\frac{\partial g}{\partial v}(0,0)\frac{D}{H}$ has no contribution to the normal kernel.

Therefore, $\delta\bar{P}_1(D,t)$ has no contribution to the kernel. The normal kernel is just the contribution from $\delta\bar{P}_2(D,t)$, therefore:

$$k_n=-\frac{2}{3}\rho(0)\pi$$

2.3.2 The overall geometric sensitivity of the on-panel case

The overall geometric sensitivity for on-panel case is the sum of the contributions from the displacement of the vertex and that of the center. The figure 2-11 shows the displacement of the vertex and the center:

As shown in the figure 2-11, $V(3)$ is perturbed in the direction of $\vec{d}$ by the distance of t, while the center $C(0)$ is perturbed in the same direction of $\vec{d}$ but the distance it goes is $\frac{t}{3}$.

And the potential at the center of the panel at t is the function of both the position of the panel and the center, written as $\bar{P}(u,v)$, with u as the distance the vertex goes and v as the distance the center goes. Then the potential at t is:

$$\bar{P}(t)=\bar{P}(u(t),v(t))$$

where $u(t)=t$ and $v(t)=\frac{1}{3}t$.

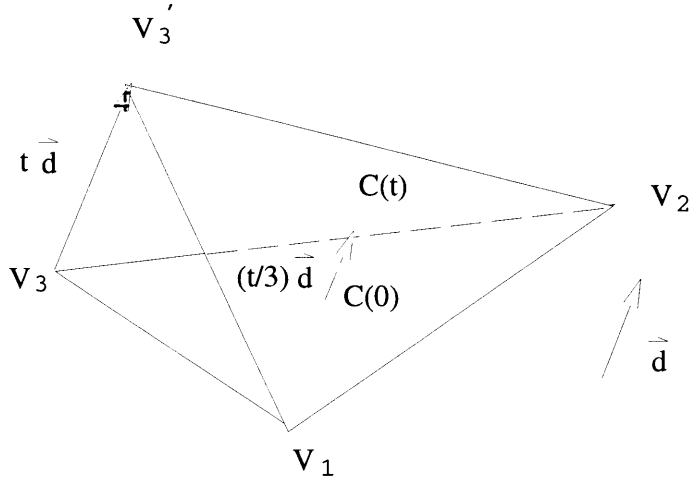

Figure 2-11: The joint displacement of the center and the vertex

The geometric sensitivity for tangential perturbation of on-panel case

For tangential perturbation, the sensitivity is just:

$$\frac{d\bar{P}(u(t),v(t))}{dt}|_{t=0} = \frac{\partial \bar{P}(0,0)}{\partial u} + \frac{\partial \bar{P}(0,0)}{\partial v} \cdot \frac{1}{3} \tag{2.16}$$

where the first term is just the potential generated by a linear dipole distribution, because the kernel is zero:

$$\frac{\partial \bar{P}(0,0)}{\partial u} = \iint_{S(0)} \frac{\epsilon \cos\theta}{r(0)^2} \rho(0) ds(0)$$

The second term, is the contribution of tangential gradient of the electrostatic field at $C(0)$:

$$\frac{\partial \bar{P}(0,0)}{\partial v} \cdot \frac{1}{3} = \frac{1}{3} \nabla_{tan} \bar{P}|_{C(0)} \bullet \vec{d}$$

So the overall tangential sensitivity is:

$$\frac{d\bar{P}(t)}{dt}|_{t=0} = \iint_{S(0)} \frac{\epsilon \cos\theta}{r(0)^2} \rho(0) ds(0) + \frac{1}{3} \nabla_{tan} \bar{P}|_{C(0)} \bullet \vec{d} \tag{2.17}$$

The geometric sensitivity for normal perturbation of the on-panel case

For normal perturbation, extra care should be taken because there is no two-sided kernel or two-sided normal gradient because of the symmetry of the electric field about the panel.

From the result of the last subsection, the one-sided sensitivity is:

$$\frac{\partial \bar{P}(0,0)}{\partial u} = \iint_{S(0)} \frac{\epsilon \cos\theta}{r(0)^2} \rho(0) ds(0) + k_n$$

where $k_n = -\frac{2}{3}\rho(0)\pi$. The derivative is evaluated at $u = 0^+$.

Because the direction of the dipole is the same as $\vec{d}$, which is normal to the panel, and the evaluation point is on the panel, the potential due to the dipole distribution is actually zero. Therefore,

$$\frac{\partial \bar{P}(0,0)}{\partial u} = -\frac{2}{3}\rho(0)\pi$$

The kernel is the same for all of the three vertices.

To compute the normal gradient of the electrical field at the original center of the panel, which is the sensitivity of the potential at the evaluation point moving from $C(0)$ off the panel in the normal direction $\vec{d}$. To have an equivalent potential sensitivity, shift the panel by the distance of t in the direction of $-\vec{d}$, fix the evaluation point at the original center, and compute the sensitivity of the potential to t. Moreover, this shift is the same as letting three vertices move in the same direction of $-\vec{d}$ by distance t. So the sensitivity of the potential at the original evaluation point $C(0)$ due to the shift of the panel is the superposition of the sensitivity of potential due to the perturbation of one vertex at a time. The sensitivity of the potential due to the displacement of any vertex of the three along $-\vec{d}$ is just the same as that along $\vec{d}$, with the value as k_n, as the result of the symmetry of the electrical filed. So the sensitivity of the potential to t is $3k_n$, or:

$$\nabla_{nor} \bar{P}|_{C(0)} = 3k_n$$

Now the overall sensitivity can be easily shown to be zero. Still use the function of the potential for the tangential case, the potential change at t is :

$$\begin{aligned}\delta\bar{P}(t) &= \bar{P}(t,\frac{t}{3}) - \bar{P}(0,0) \\ &= (\bar{P}(t,\frac{t}{3}) - \bar{P}(t,0)) + (\bar{P}(t,0) - \bar{P}(0,0))\end{aligned}$$

The first term in the equation is the potential change of the case that the evaluation point is moving back into the panel, in the direction that is approaching normal direction of the panel as t approaches 0. The second term is the potential change given the evaluation point is fixed at $C(0)$ while the panel is perturbed in the normal direction. The sensitivity of the two terms are:

$$\lim_{t\to 0^+} \frac{1}{t}(\bar{P}(t,\frac{t}{3}) - \bar{P}(t,0)) \tag{2.18}$$

$$= -\nabla_{nor}\bar{P}|_{C(0)} \cdot \frac{1}{3} = -k_n \tag{2.19}$$

$$\tag{2.20}$$

and

$$\lim_{t\to 0^+} \frac{1}{t}(\bar{P}(t,0) - \bar{P}(0,0)) = k_n$$

Therefore,

$$\lim_{t\to 0^+} \frac{\delta P(t)}{t} = 0$$

Since this relation holds for both sides of derivative, it can be written as:

$$\frac{d\bar{P}(t)}{dt} = 0$$

2.3.3 Conclusion of the electrostatic geometric sensitivity of the potential generated by a panel charged with uniform source distribution

From the description in the preceeding sections, the electrostatic geometric sensitivity of the potential generated by a charged panel is:

1. For off-panel case, the sensitivity is just the potential at the evaluation point due to a linear dipole distribution:

$$\frac{d\bar{P}(t)}{dt}|_{t=0} = \iint_{S(0)} \frac{\epsilon \cos\theta}{r(0)^2} \rho(0) ds(0)$$

2. For on-panel case,

   (a) The sensitivity for tangential perturbation in the on-panel case is

$$\frac{d\bar{P}(t)}{dt}|_{t=0} = \iint_{S(0)} \frac{\epsilon \cos\theta}{r(0)^2} \rho(0) ds(0) + \frac{1}{3} \nabla_{tan} \bar{P}|_{C(0)} \bullet \vec{d}$$

   (b) The sensitivity for normal perturbation in the on-panel case is 0.

2.4 Closed form analytic formulas

In this section, closed form analytic formulas will be derived for:

1. The potential due to a linear dipole distribution

2. The gradient of the electrostatic field due to the uniform source distribution

Both the potential and the gradient are computed at the original evaluation point. The gradient of the normal direction of the on-panel case does not exist and is neglected.

2.4.1 The simplification of the formula into 1-D integration

For simplicity, the triangle is put in the position on $Z = 0$ plane as shown in the figure 2-12, where V_3 is the vertex under perturbation. V_1 is at $(0, 0, 0)$, V_2 at $(\xi_2, 0, 0)$, and V_3 is at $(\xi_3, h, 0)$. The length of the height on V_2V_3 is h. Z direction is normal to the panel. For an arbitrary point $A(\xi, \eta, 0)$ in the triangle, the linearly

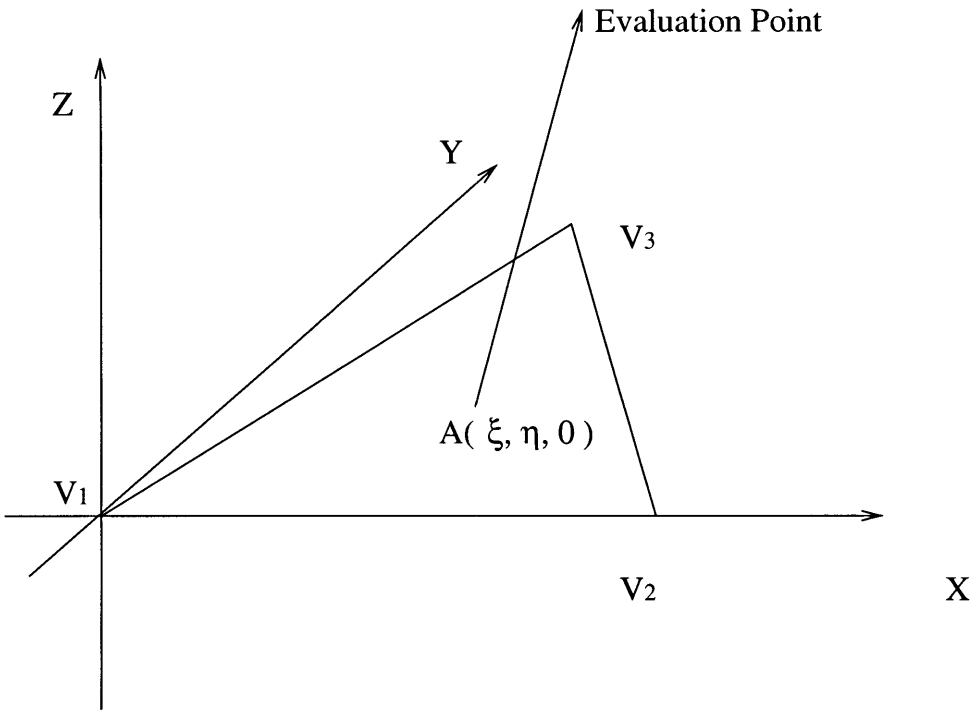

Figure 2-12: The position of the panel for computation

varying coefficient for the dipole distribution is $\epsilon = \frac{\eta}{h}$. The evaluation point is at (x, y, z).

According to Newman's paper [4], the potential due to a uniformly distributed source charge with unit density is:

$$\Psi = \iint \frac{1}{r} d\xi d\eta$$

where

$$r = \sqrt{(x-\xi)^2 + (y-\eta)^2 + z^2}$$

and the potential due to a uniform normal dipole distribution of unit density is:

$$\Phi = \iint \frac{\partial}{\partial \zeta}(\frac{1}{r})|_{\zeta=0} d\xi d\eta$$

Both integrations should be computed over the whole panel.

Assume the original charge density on the panel is ρ, then the potential at evaluation point (x, y, z) due to the linear dipole distribution in X , Y and Z directions are:

$$
\begin{aligned}
\Phi_{LX} &= \rho \iint \frac{\eta}{h} \frac{\partial}{\partial \xi}(\frac{1}{r}) d\xi d\eta \\
&= \frac{\rho}{h} \int \eta (\int \frac{\partial}{\partial \xi}(\frac{1}{r}) d\xi) d\eta \\
&= \frac{\rho}{h} (\int_{V_2 \to V_3} \frac{\eta}{r} d\eta - \int_{V_1 \to V_3} \frac{\eta}{r} d\eta)
\end{aligned}
$$

$$
\begin{aligned}
\Phi_{LY} &= \rho \iint \frac{\eta}{h} \frac{\partial}{\partial \eta}(\frac{1}{r}) d\eta d\xi \\
&= \frac{\rho}{h} \int (\int (\frac{\partial}{\partial \eta}(\frac{\eta}{r}) - \frac{1}{r}) d\eta) d\xi \\
&= \frac{\rho}{h} ((- \int_{V_2 \to V_3} \frac{\eta}{r} d\xi + \int_{V_1 \to V_3} \frac{\eta}{r} d\xi) - \Psi)
\end{aligned}
$$

$$
\begin{aligned}
\Phi_{LZ} &= \rho \iint \frac{\eta}{h} \frac{\partial}{\partial \zeta}(\frac{1}{r}) d\xi d\eta \\
&= \frac{\rho}{h} (z \iint \frac{\eta}{r^3} d\xi d\eta) \\
&= \frac{\rho}{h} (z \iint \frac{(\eta - y) + y}{r^3} d\xi d\eta) \\
&= \frac{\rho}{h} (y \iint \frac{z}{r^3} d\xi d\eta - z \iint \frac{\partial}{\partial \eta}(\frac{1}{r}) d\xi d\eta) \\
&= \frac{1}{h} (\rho y \Phi + z \nabla_Y \bar{P}|_C(0))
\end{aligned}
$$

The integration of Φ_{LX} and Φ_{LY} have been broken into the directional integration over the sides of the triangle. The direction of the integration has been aligned to be off the X axis for further simplification.

The gradient formula can also be rewritten in the same way:

$$
\begin{aligned}
\nabla_X \bar{P} &= -\rho \iint \frac{\partial}{\partial \xi}(\frac{1}{r}) d\xi d\eta \\
&= \rho (- \int_{V_2 \to V_3} \frac{1}{r} d\eta + \int_{V_1 \to V_3} \frac{1}{r} d\eta)
\end{aligned}
$$

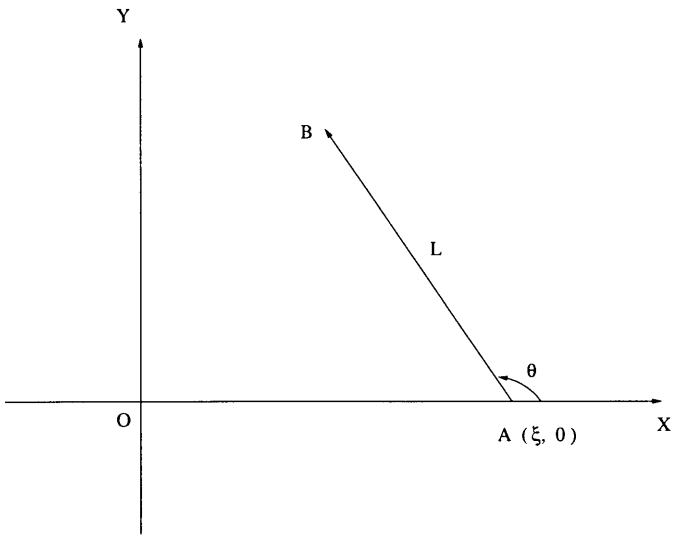

Figure 2-13: The domain of the 1-D directional integration

$$\begin{aligned}
\nabla_Y \bar{P} &= -\rho \iint \frac{\partial}{\partial \eta}(\frac{1}{r}) d\eta d\xi \\
&= \rho(\int_{V_2 \to V_3} \frac{1}{r} d\xi - \int_{V_1 \to V_3} \frac{1}{r} d\xi + \int_{V_1 \to V_2} \frac{1}{r} d\xi)
\end{aligned}$$

$$\begin{aligned}
\nabla_Z \bar{P} &= -\rho \iint \frac{\partial}{\partial \zeta}(\frac{1}{r}) d\xi d\eta \\
&= -\rho \Phi
\end{aligned}$$

2.4.2 Closed analytic form

Closed analytic form of Φ and Ψ has been derived in the paper [4], and the 1-D integrations in the equations above can also be turned into closed analytic form.

There are two types of integrations involved in these equations, one is the integration of $\frac{1}{r}$, another is the integration of $\frac{\eta}{r}$. Both the integrations are calculated through a directional line starting from a point at the X axis.

As shown in figure 2-13, the domain of most of the 1-D integrations for the equations can be described as a line L with a defined direction. The starting point

is A with coordinates $(\xi, 0)$, θ is the angle between the direction of the line and the positive direction of the X axis, and Y coordinate of the ending point B is h. Two functions can be defined as the result of the integration, which will resolve all of the integrations in the equations except $\int_{V_1 \to V_2} \frac{1}{r} d\xi$.

Define

$$f(\xi, \theta, h) = \int_L \frac{\partial}{\partial \eta}(\frac{\eta}{r}) d\eta$$

and

$$g(\xi, \theta, h) = \int_L \frac{\partial}{\partial \eta}(\frac{1}{r}) d\eta$$

then it follows that:

$$\int_L \frac{\partial}{\partial \eta}(\frac{\eta}{r}) d\xi = f(\xi, \theta, h) \cot \theta$$

and

$$\int_L \frac{\partial}{\partial \eta}(\frac{1}{r}) d\xi = g(\xi, \theta, h) \cot \theta$$

which resolve the terms of integration over ξ.

The analytic form of $g(\xi, \theta, h)$ and $f(\xi, \theta, h)$ can be derived jointly as:

$$g(\xi, \theta, h) = \frac{1}{\sqrt{a}} \ln \frac{2ah + b + 2\sqrt{a} R_B}{b + 2\sqrt{a} R_A} \tag{2.21}$$

$$f(\xi, \theta, h) = \frac{1}{a}(R_B - R_A) - \frac{b}{2a} g(\xi, \theta, h) \tag{2.22}$$

where R_A and R_B are distance from the (x, y, z) to the starting point and ending point of L, respectively, and

$$a = \csc^2 \theta$$

$$b = 2(\xi - x) \cot \theta - 2y$$

Finally, define:

$$\omega(\xi_2) = \int_{V_1 \to V_2} \frac{1}{r} d\xi$$

its closed analytic form is:

$$\omega(\xi_2) = \frac{1}{\sqrt{a}} \ln \frac{2a\xi_2 + b + 2\sqrt{a}R_2}{b + 2\sqrt{a}R_1} \tag{2.23}$$

where $a = 1$, $b = -2x$, and R_1, R_2 are the distance from (x, y, z) to V_1 and V_2, respectively.

Denote θ_{23} as the angle of the direction of the line from V_2 to V_3 with the positive direction of X axis, and θ_{13} as that of the line from V_1 to V_3, then the closed form analytic formulas for linear dipole distribution and the gradient are:

$$\begin{aligned}
\Phi_{LX} &= \frac{\rho}{h}(f(\xi_2, \theta_{23}, h) - f(0, \theta_{13}, h)) \\
\Phi_{LY} &= \frac{\rho}{h}(-f(\xi_2, \theta_{23}, h)\cot\theta_{23} + f(0, \theta_{13}, h)\cot\theta_{13} - \Psi) \\
\Phi_{LZ} &= \frac{1}{h}(\rho y\Phi + z\ \nabla_Y \bar{P}|_{C(0)})
\end{aligned}$$

and:

$$\begin{aligned}
\nabla_X \bar{P}|_{C(0)} &= \rho(-g(\xi_2, \theta_{23}, h) + g(0, \theta_{13}, h)) \\
\nabla_Y \bar{P}|_{C(0)} &= \rho(g(\xi_2, \theta_{23}, h)\cot\theta_{23} - g(0, \theta_{13}, h)\cot\theta_{13} + \omega(\xi_2)) \\
\nabla_Z \bar{P}|_{C(0)} &= -\rho\Phi
\end{aligned}$$

The closed form analytic formula of Ψ and Φ is in the paper of Newman [4].

Chapter 3

Fast electrostatic geometric sensitivity algorithm

3.1 Direct computation of electrostatic geometric sensitivity for a system of N charged panels

Assume that in the piecewise constant collocation scheme for applications, there are N triangular panels as shown in figure 3-1.

The evaluation points are the center of the panels, $C_1, C_2, \ldots, C_N$. It is assumed that no center of any panel is on another panel and every panel has constant net charge which is uniformly distributed over the panel during the perturbation.

Then the potential at the evaluation points is the function of the coordinates of the panels, $\bar{P}(u)$, where u is the vector of the $9N$ coordinate of the $3N$ vertices. The sensitivity matrix J of the potential to the coordinates of the vertices is $J = \frac{\partial \bar{P}}{\partial u}$, with N rows and $9N$ columns. $\frac{\partial \bar{P}_i}{\partial u_j}$ is the sensitivity of the potential at C_i to the perturbation of the vertex with u_j as one coordinate along the positive direction of the axis of u_j.

The sensitivity block of the potential at C_i to the perturbation of the n-th panel

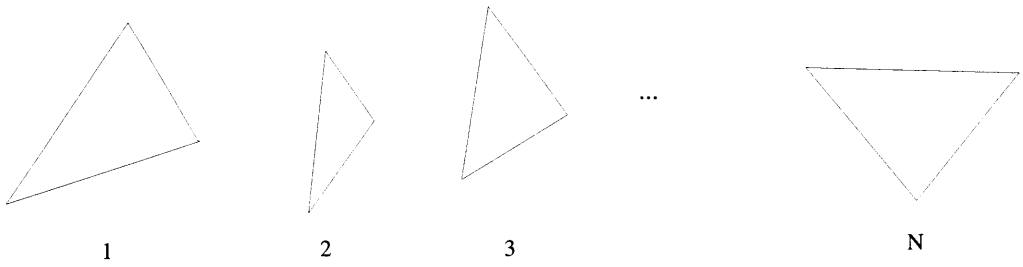

Figure 3-1: A system of charged panels

is $\frac{\partial \bar{P}_i}{\partial u_j}$, $j = 9n+1, 9n+2, \ldots, 9n+9$.

If the vertices are perturbed with direction and distance specified by the coordinate vector of $\hat{u}$, then the electrostatic geometric sensitivity is

$$\frac{d}{dt}\bar{P}(u+\hat{u}t)|_{t=0} = \frac{\partial \bar{P}}{\partial u}\hat{u} \tag{3.1}$$

Consider the sensitivity of the potential at C_i, which is

$$\sum_{j=1}^{9N} \frac{\partial \bar{P}_i}{\partial u_j}\hat{u}_j$$

The terms of the sum can be grouped into a cross term and a self term according to j. Define two sets by $A = \{9i+1, 9i+2, \ldots, 9i+9\}$, and $B = \{1, 2, \ldots, 9N\} - A$, then:

$$\sum_{j=1}^{9N} \frac{\partial \bar{P}_i}{\partial u_j}\hat{u}_j = S_{cross} + S_{self}$$

where

$$S_{self} = \sum_{j\in A} \frac{\partial \bar{P}_i}{\partial u_j}\hat{u}_j$$

$$S_{cross} = \sum_{j\in B} \frac{\partial \bar{P}_i}{\partial u_j}\hat{u}_j$$

Since A is the set of the index of components of u that is associated with the panel i, and B is the set of the index of the components of u that is associated with all the

other panels, cross term S_{cross} is the sum of the contributions from the sensitivity of $\bar{P}_i$ due to the perturbation of vertices of the panels other than the i-th one, while self term S_{self} is the sum of the contributions from the sensitivity of $\bar{P}_i$ due to the perturbation of vertices of the i-th panel itself.

Computation of the cross and self terms needs the result from the last chapter:

1. Computation of the cross term.

   Consider the contribution to the cross term from the j-th vertex, $\frac{\partial \bar{P}_i}{\partial u_j}\hat{u}_j$, where $j \in B$. $\frac{\partial \bar{P}_i}{\partial u_j}$ is just the sensitivity of the potential at C_i due to the perturbation of the vertex of a charged panel associated with u_j. And because C_i is off the panel that is associated with u_j, the sensitivity of the potential is just the potential of a linear dipole distribution in the direction of the positive direction of axis of u_j. $\hat{u}_j$ is a scale of the contribution to the overall sensitivity.

   In the computation of the potential at C_i due to the linear dipole distribution over the other panels, a dipole distribution in the direction of global axis can be decomposed into the dipoles in the normal or tangential directions of panels, for which closed analytic formulas have been derived in the last chapter.

2. Self term.

   The Self term S_{self} is the sensitivity of $\bar{P}_i$ to the perturbation of the vertices of the i-th panel itself. S_{self} can be decomposed further into two parts, according to the panels generating the potential.

   The potential $\bar{P}_i$ can be decomposed into the contribution from the electrical field generated by the i-th panel itself and that from the electrical field generated by the other panels:

$$\bar{P}_i = \bar{P}_{i_{ss}} + \bar{P}_{i_{sc}}$$

where $\bar{P}_{i_{ss}}$ is the potential generated at C_i by the i-th panel itself, and $\bar{P}_{i_{sc}}$ is the potential generated at C_i by all the other panels.

Then the self term S_{self} can be decomposed into self-self term S_{ss} and self-cross term S_{sc}:

$$S_{self} = S_{ss} + S_{sc}$$

where

$$S_{ss} = \sum_{j \in A} \frac{\partial \bar{P}_{i_{ss}}}{\partial u_j} \hat{u}_j$$

and

$$S_{sc} = \sum_{j \in A} \frac{\partial \bar{P}_{i_{sc}}}{\partial u_j} \hat{u}_j$$

The self-self term and self-cross term can also be computed with the results of the last chapter:

(a) Self-self term S_{ss}.

Since:

$$S_{ss} = \sum_{j \in A} \frac{\partial \bar{P}_{i_{ss}}}{\partial u_j} \hat{u}_j$$

consider $\frac{\partial \bar{P}_{i_{ss}}}{\partial u_j} \hat{u}_j$, where $j \in A$. $\frac{\partial \bar{P}_{i_{ss}}}{\partial u_j}$ is the sensitivity of the potential at C_i generated by the i-th panel itself to the perturbation of one vertex of the panel. This is just the electrostatic geometric sensitivity for evaluation-point-on-panel case that has been covered in the last chapter. As in the cross term computation, $\hat{u}_j$ is a scale of the contribution to the overall sensitivity.

(b) Self-cross term.

$$S_{sc} = \sum_{j \in A} \frac{\partial \bar{P}_{isc}}{\partial u_j} \hat{u}_j$$

Consider $\frac{\partial \bar{P}_{isc}}{\partial u_j} \hat{u}_j$. $\frac{\partial \bar{P}_{isc}}{\partial u_j}$ is the sensitivity of the potential at the center of the i-th panel generated by all the other panels to the perturbation of one vertex of the i-th panel. So:

$$\frac{\partial \bar{P}_{isc}}{\partial u_j} = \frac{1}{3} \nabla \bar{P}_{isc}|_{C_i} \bullet \vec{u}_j$$

where $\vec{u}_j$ is a unit length vector in the positive direction of the axis of u_j, $\nabla \bar{P}_{isc}$ is the sum of the gradient of the electrical field generated by the panels other than the i-th one, which can be computed with the result of the last chapter.

Again, $\hat{u}_j$ is a scale of the contribution to the overall sensitivity.

With the method described above based on the one-panel sensitivity analysis, all the derivatives involved can be computed.

For large numbers of panels, the direct method is too slow. Fast algorithm can be developed to accelerate the sensitivity computation by combining the formulas of one-panel sensitivity with Precorrected FFT method.

3.2 The Precorrected FFT method for fast potential computation

The Precorrected FFT method is a general fast algorithm for potential computation of 3-D structures. It will be briefly described here for simplicity. A detailed description of this method is in [5].

Take the system of charged panels described in the last section as an example, the steps of the Precorrected-FFT algorithm to evaluate the potential at the center of each of the panels can be summarized as:

1. Set up a uniform 3-D grid to cover the whole domain of the panels.

2. Do forward projection of the source charge onto the grid points. For every panel, project the panel's charge onto the nearby grid points so as to approximately represent the electrical field the panel's charge generates far from the panel. The grid charge vector $\hat{q}$ is:

$$\hat{q} = Wq$$

where W is the forward projection matrix, q is the vector of panel charges.

3. Then the potential at the grids in the whole space due to the grid charges is calculated by the FFT algorithm:

$$\hat{\Psi} = H\hat{q} = HWq$$

where H is the convolution matrix.

4. The potential at the center of the panels is interpolated by the backward projection from the nearby grid:

$$\Psi_G = V^T\hat{\Psi} = V^THWq$$

where V^T is the interpolation matrix.

5. The potential due to the nearby panels is calculated directly, and the contribution due to the grid method is subtracted:

$$\bar{P} = \bar{P}_d + \Psi_G - \Psi_{Gn}$$

where $\bar{P}$ is the potential estimation, $\bar{P}_d$ is the potential contribution from the direct computation, and Ψ_{Gn} is the potential contribution of the nearby panels inaccurately computed using the grid.

The Precorrected FFT accelerated potential estimation is faster than the direct estimation method because it employs the grid to represent the charge for the field

the charge generates far from it, and FFT accelerates the grid potential computation. Moreover, if the potential at the centers of the panels is to be computed for several sets of charges on the panels, which is necessary in FFTCAP, further acceleration of the potential estimation can be achieved by the implementation of the Precorrected-FFT method with two stages, a setup stage and an evaluation stage. In the setup stage, the forward projection coefficients for unit charge are evaluated and stored. Backward projection coefficients and the direct interaction coefficients are also computed and stored in the setup stage. In the evaluation stage, the coefficients are multiplied with the real charge to get the grid representation for FFT computation. The overhead of the setup is large, but the evaluation stage is very fast. This is exactly the reason of the high speed of FFTCAP.

3.3 Fast algorithm for electrostatic geometric sensitivity computation

In terms the electrostatic geometric sensitivity defined by equation 3.1, the sensitivity of the potential at the center of one panel is the the sum of a cross term and a self term. The computational complexity of the cross term is dominant because it is the sum of the contributions of all the other panels, which has been shown to be the potential generated by linear dipole distributions induced by perturbation. Therefore, the computation of sensitivity due to the cross terms is just a potential computation. Based on this fact, the linear dipole formula can be combined with Precorrected FFT method for fast computation of electrostatic geometric sensitivity as defined in equation 3.1.

The new algorithm has a structure similar to the fast potential computation algorithm of Precorrected FFT method.

Fast algorithm for electrostatic geometric sensitivity computation

1. Set up a uniform 3-D grid to cover the whole domain of the panels.

2. Forward projection of the linear dipole distributions onto the grid points. There are 9 independent linear dipoles induced and scaled by the perturbation for every panel. The grid charge vector $\hat{q}$ is:

$$\hat{q} = W\hat{u}$$

where W is the forward projection matrix, $\hat{u}$ is the perturbation vector of the vertices.

3. Then the potential at the grids in the whole space due to the grid charges is computed by the FFT algorithm

$$\hat{\Psi} = H\hat{q} = HW\hat{u}$$

where H is the convolution matrix.

4. The potential at the center of the panels is interpolated by the backward projection from the nearby grid

$$\Psi_G = V^T\hat{\Psi} = V^T HW\hat{u}$$

where V^T is the interpolation matrix.

5. The potential due to the nearby panels is calculated directly, and the contribution due to the grid method is subtracted, as in

$$\bar{P} = \bar{P}_d + \Psi_G - \Psi_{Gn}$$

Here $\bar{P}$ is the potential estimated, which is actually a sensitivity estimation, $\bar{P}_d$ is the potential contribution from the direct computation, and Ψ_{Gn} is the potential contribution of the nearby panels inaccurately computed using the grid.

The direct calculation here has three parts:

1. Cross term that corresponds to nearby interaction. This can be resolved by linear dipole formula.

2. Self-self term can be computed by the on-panel case sensitivity formula.

3. Self-cross term is the sensitivity to the perturbation of the vertices of the same panel due to the electrostatic gradient of the field generated by all the other panels. The gradient at the center of all panels can be computed in parallel by running the algorithm without the self term:

   Assume x is the unit length vector of the direction for which the gradient is to be computed, then construct a perturbation vector v with $-x$ as the component of every vertex. Because the self term is ignored in the computation, the actual perturbation is that for every panel, all the other panels are shifted in the opposite direction of x with the the panel itself fixed.

   With the fact that potential is just dependent on the relative position of the charge and the evaluation point, The sensitivity of $\frac{d}{dt}\bar{P}(u+vt)|_{t=0}$ computed without self term at the center of every panel is just the gradient along x of the field generated by all the other panels.

   The advantage of running the no-self-term algorithm to compute the gradient is that the gradient at the center of every panel due to the electrostatic field generated by the other panels is computed in parallel.

Similar to the potential computation by Precorrected FFT method, if the sensitivity to many perturbations at the same position of the system needs to be computed, acceleration of the algorithm can also be achieved by the implementation with two stages, a slow setup stage and a fast evaluation stage. In the setup stage, the coefficients for forward projection of the linear dipole distribution induced by unit perturbations are estimated and stored as well as the backward projection coefficients. In the evaluation stage, the perturbation is multiplied with the projection coefficients to

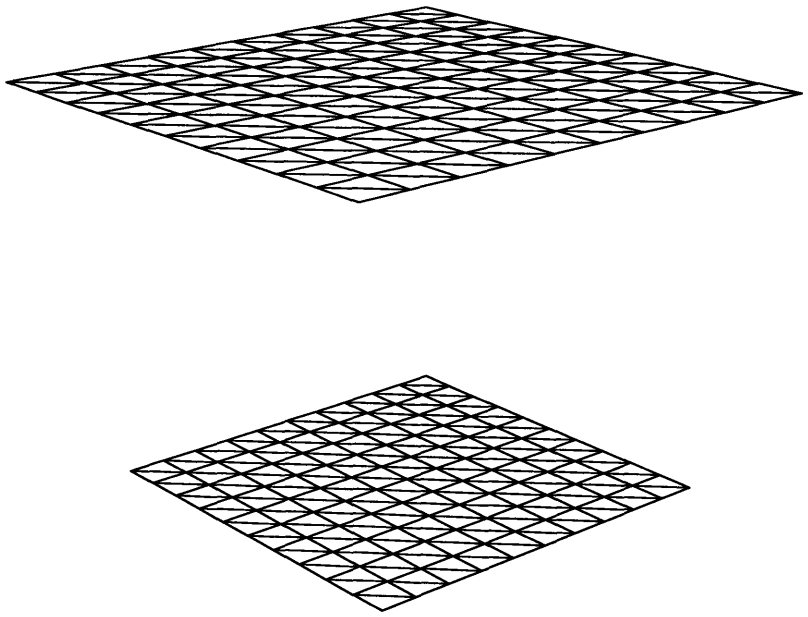

Figure 3-2: The system of panels for test

generate grid charge. The whole procedure is quite similar to the potential computation in FFTCAP [5], except that the charge to be projected onto the grid is a linear dipole distribution instead of a source distribution. In the evaluation stage, the fast algorithm generates the potential change vector, $\frac{\partial P(u)}{\partial u}\hat{u}$, for the perturbation vector $\hat{u}$.

3.4 An example of the accuracy of the algorithm

An example to show the accuracy of the algorithm is a system with 400 panels on two parallel squares with side length of 10 and distance of 20 , as shown in the figure 3-2.

For perturbations with a direction and magnitude specified by the vector $\hat{u}$, the geometric sensitivity is $\frac{\partial \bar{P}}{\partial u}\hat{u}$. The sensitivity is computed by the fast algorithm described above, and compared with the direct method of evaluating the matrix $\frac{\partial P(u)}{\partial u}$ analytically.

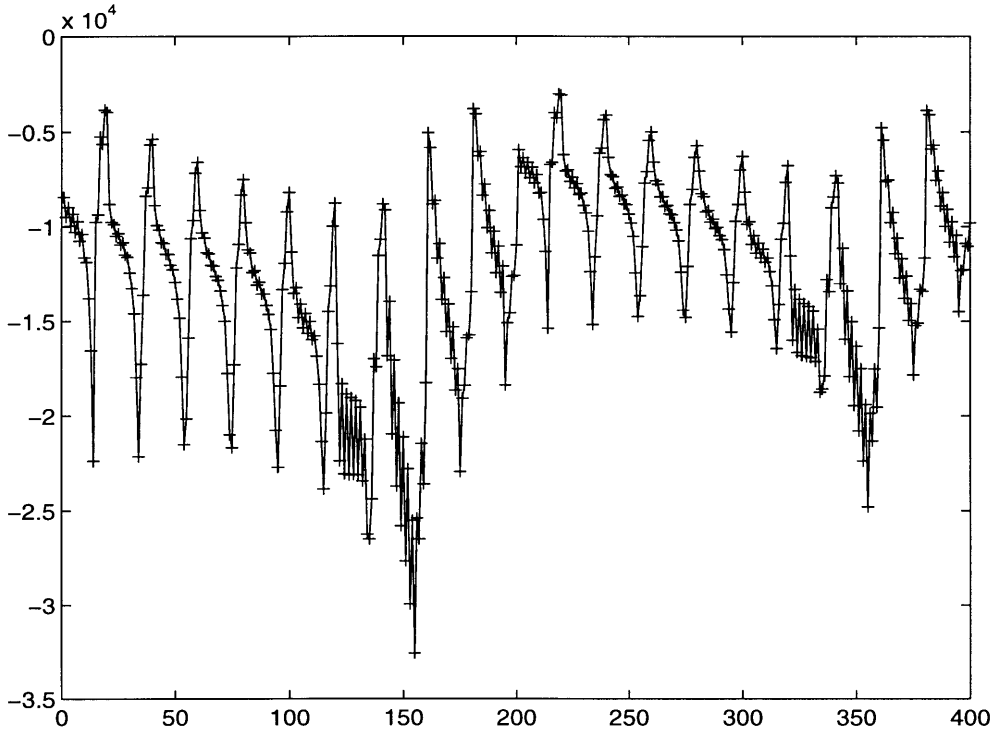

Figure 3-3: The accuracy of the result by the fast algorithm

In figure 3-3, the results from using both methods for the case of $\hat{u} = [1, 2, \cdots, 3600]$ are shown.

The X axis in the figure is the index of the evaluation point, which is the center of the panel. The Y axis is the sensitivity estimated. The solid line is the result of the direct method and the line of '+' is the result of the fast algorithm of geometric sensitivity computation. As is clear from the graph, the results are nearly identical, and the computed maximum relative error for this $\hat{u}$ is less than 0.002.

The computational speed will be addressed in the next chapter.

Chapter 4

Applications of the fast algorithm for electrostatic geometric sensitivity computation

As described in chapter one, the the fast algorithm for electrostatic geometric sensitivity computation can be employed to accelerate the solving of the coupled electromechnical equations, and to compute the geometric sensitivity of capacitance due to geometric perturbation efficiently. The following section is a detailed description on the application of the algorithm to the geometric sensitivity analysis of capacitance.

4.1 Application of the fast electrostatic geometric sensitivity computation algorithm to the geometric sensitivity analysis of capacitance

4.1.1 Capacitance computation by numerical method

The capacitance of an M-conductor geometry can then be written as an $M \times M$ symmetric matrix C, where the entry C_{ij} represents capacitive coupling between conductors j and i. The j-th column of C, or the capacitance associated with the j-th conductor, is just the surface charges on each conductor produced by setting conductor j to one volt while grounding the rest.

A standard numerical approach to solve the charge is by piecewise constant collocation scheme [5, 3]. In this scheme, the conductor surfaces are discretized into n small panels, and uniform charge distribution is assumed on the panels. A dense linear system can be written to relate the charge on the panels to the potential at the center of the panels:

$$Pq = \bar{P} \tag{4.1}$$

where $P \in \mathbf{R}^{n \times n}$, $q \in \mathbf{R}^n$ is the vector of panel charges to be solved, $\bar{P} \in \mathbf{R}^n$ is the vector of known panel potentials, and P_{ij} is the potential generated at the center of the i-th panel by unit charge over the j-th panel.

To solve C_j, the column of capacitance associated with the j-th conductor, just set to one volt the components of $\bar{P}$ that is the potential at the center of the panels of the j-th conductor while grounding the other components, solve the linear system and sum the charges of the panels that belong to the same conductor. The summing operation is the multiplication of a summing matrix with the computed charge vector.

Denote $\bar{P}^j$ as the potential vector associated with the computation of C_j, $\bar{q}^j$ as the vector of panel charges derived by solving equation 4.1, and S as the transpose

of the summing matrix. The i-th column of S, S^i, is the summing vector for the capacitance of the i-th conductor. The components of S^i are 1 for the panels of the i-th conductor and zero for all the other components. With these definitions, the method of capacitance computation described above can be summarized by:

$$\begin{aligned} Pq^j &= \bar{P}^j \\ C_j &= S^T q^j \end{aligned}$$

4.1.2 Geometric sensitivity of capacitance under numerical scheme

In the geometric sensitivity analysis by the collocation scheme, the capacitance matrix $C(u)$ is dependent on the position of every vertex of the panels, specified by the vector u. The degree of freedom of u is $9n$.

Similar to the electrostatic geometric sensitivity of the potential of a system of charged panels, the geometric sensitivity of the capacitance to perturbation $\hat{u}$ at position u can be defined as:

$$\frac{d}{dt}\bar{C}(u+\hat{u}t)|_{t=0} = \frac{\partial C(u)}{\partial u}\hat{u} \tag{4.2}$$

One way to compute the geometric sensitivity is by finite difference method. Consider the sensitivity of $C_j(u)$. Both $C_j(u)$ and $C_j(u+\hat{u}t)$ can be computed by the capacitance computation method described in the last subsection. Then the sensitivity is:

$$\frac{d}{dt}\bar{C}(u+\hat{u}t)|_{t=0} \approx \frac{1}{t}\left(C_j(u+\hat{u}t) - C_j(u)\right)$$

However, this method suffers from two problems:

1. Although FFTCAP and FASTCAP can be used to accelerate the capacitance computation, this method will be slow when the sensitivity to a lot of vectors is to be computed because a new setup is necessary for every perturbation vector.

2. The value of t is difficult to determine. If it is not small enough, the estimation might not reflect the sensitivity well. But if it is too small, the small change of the capacitance might be corrupted by numerical errors.

Another approach is a derivative method that can be accelerated by the fast algorithm of electrostatic geometric sensitivity computation. The capacitance during the perturbation is determined by:

$$P(u+\hat{u}t)q^j(u+\hat{u}t) = \bar{P}^j \tag{4.3}$$

$$C_j(u+\hat{u}t) = S^T q^j(u+\hat{u}t) \tag{4.4}$$

By differentiating the first equation with respect to t, an equation for the sensitivity of the charge, $\frac{\partial q^j(u)}{\partial u}\hat{u}$, can be derived as:

$$P(u)(\frac{\partial q^j(u)}{\partial u}\hat{u}) = -\frac{\partial \bar{P}_{q^j(u)}(u)}{\partial u}\hat{u} \tag{4.5}$$

And the sensitivity of the capacitance can be related to the sensitivity of the charge by differentiating the second equation:

$$\frac{d}{dt}C_j(u+\hat{u}t)|_{t=0} = S^T(\frac{\partial q^j(u)}{\partial u}\hat{u}) \tag{4.6}$$

It is obvious that the expensive computation is solving for the charge sensitivity in equation 4.5. The right hand side of the charge sensitivity equation, $-\frac{\partial \bar{P}_{q^j(u)}(u)}{\partial u}\hat{u}$, is just the electrostatic geometric sensitivity due to the perturbation $\hat{u}$ while the charge over the panels is $q^j(u)$. This can be computed by the fast algorithm for electrostatic geometric sensitivity computation.

With the right hand side resolved, the sensitivity of the charge vector q^j can be resolved by solving the linear equations of 4.5. The solving is the same as solving the charge of the panels with the potential vector given as $-\frac{\partial \bar{P}_{q^j(u)}(u)}{\partial u}\hat{u}$. Therefore, GMRES can be applied and Precorrected FFT method can be used for acceleration of the matrix-vector product.

It should be noted that the sensitivity is evaluated at a position given by u, and in the computation of the right hand side of the charge sensitivity equation, which is the electrostatic geometric sensitivity due to the perturbation $\hat{u}$, the charge on the panels should be set to the charge computed at position u with the potential given by $\bar{P}^j$.

The derivative method alleviates the problems encountered in the finite difference method:

1. Because the electrostatic geometric sensitivity of the system is evaluated at the same position, only one setup is necessary for the fast algorithm for electrostatic geometric sensitivity computation. Meanwhile, only one setup is necessary for the Precorrected- FFT method for the acceleration of the GMRES solving of the charge sensitivity equation. Therefore, if the sensitivity of large amount of perturbation vectors is to be computed, the derivative method will be much faster than the finite difference method.

2. Because it is a method based on the analytic computation of derivative, there is no problem of choosing step size.

4.1.3 Some examples of computation for geometric sensitivity of capacitance

Accuracy of the derivative method

A two by two bus structure shown in figure 4-1 is used for geometric sensitivity analysis of capacitance.

The test perturbation vector is set to move the conductor $1, 2, 3, 4$ by the shift all in the direction of $(1, 1, 1)$ but the magnitude of the shift of the conductors are $1, 2, 3, 4$, respectively. By finite difference method with the step size carefully set at 10^{-5}, the sensitivity matrix of the capacitance to the perturbation is shown in table 4.1.

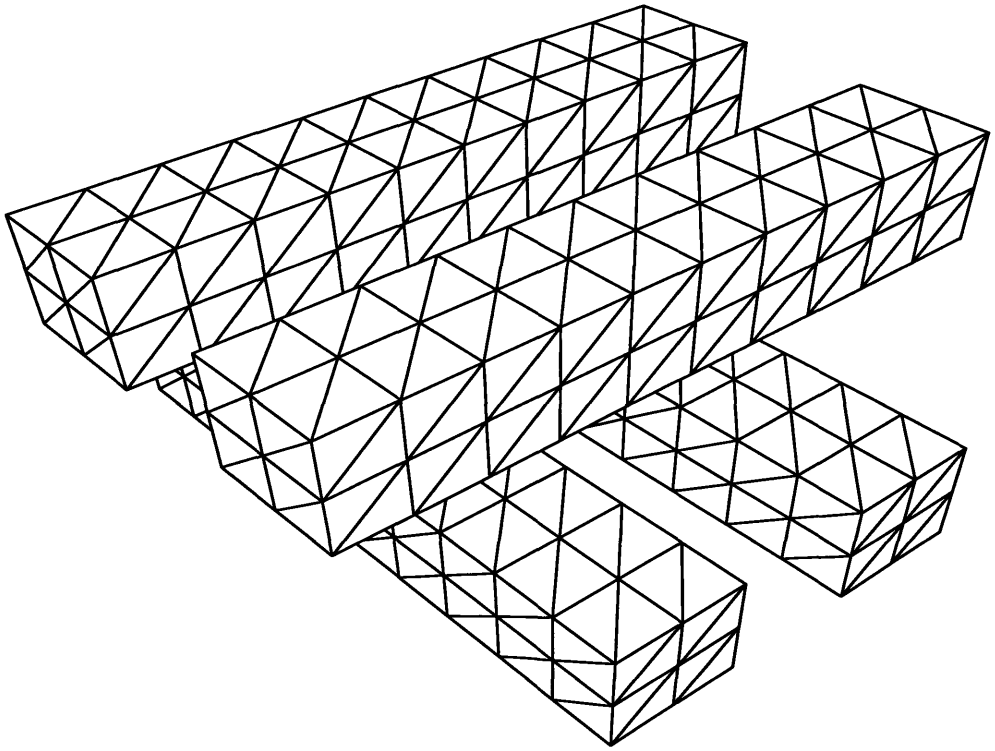

Figure 4-1: Two by two bus structure for capacitance sensitivity analysis

The sensitivity matrix of the capacitance computed by the derivative method is in table 4.2.

The two methods produce similar result. However, the result of the finite difference method varies much with the step size the method takes.

The sensitivity of C_{12} computed at different step size is shown in table 4.3.

From this table, the capacitance sensitivity computed by finite difference method

-3.59782167	0.03694578	1.31372436	2.86507031
0.03687934	-1.89402010	0.29686955	1.46009990
1.31479168	0.29972038	-2.32937557	0.65164125
2.86497775	1.45730613	0.65525497	-4.14570326

Table 4.1: Capacitance sensitivity computed by the finite difference method

-3.59562388	0.03522728	1.31330938	2.86707393
0.03510792	-1.89512666	0.29750389	1.46210316
1.31309726	0.29753646	-2.32636602	0.65313898
2.86703480	1.46207482	0.65234289	-4.15419548

Table 4.2: Capacitance sensitivity computed by the derivative method

step	sensitivity of C_{12}
10^{-2}	0.05492925
10^{-3}	0.03999656
10^{-5}	0.03687934
10^{-8}	0.01845206

Table 4.3: Dependence of the finite difference method on the step size

is very sensitive to the step size.

Speed of the derivative method

The derivative method is significantly faster than the finite difference method if the capacitance sensitivity to many perturbation vectors needs to be computed. For a detailed illustration of the speed difference of the two method, consider a more practical example of a three-by-three bus shown in figure 4-2.

Assume the sensitivity of C_{55}, the self capacitance of the conductor five, to the seventeen process variations needs to be computed. The time for the finite difference method to finish the computation is:

$$t_{dir} \approx (17+1) \times (t_{fsp} + t_g) = 18 \times 4.380071 \approx 86.04 sec$$

where $t_{fsp} = 2.475136\ sec$ is the setup time of Precorrected FFT method for potential evaluation, $t_g = 1.904935\ sec$ is the time to solve the linear system for charge at given potential by GMRES method after the setup.

For derivative method, only one setup is necessary for electrostatic geometric

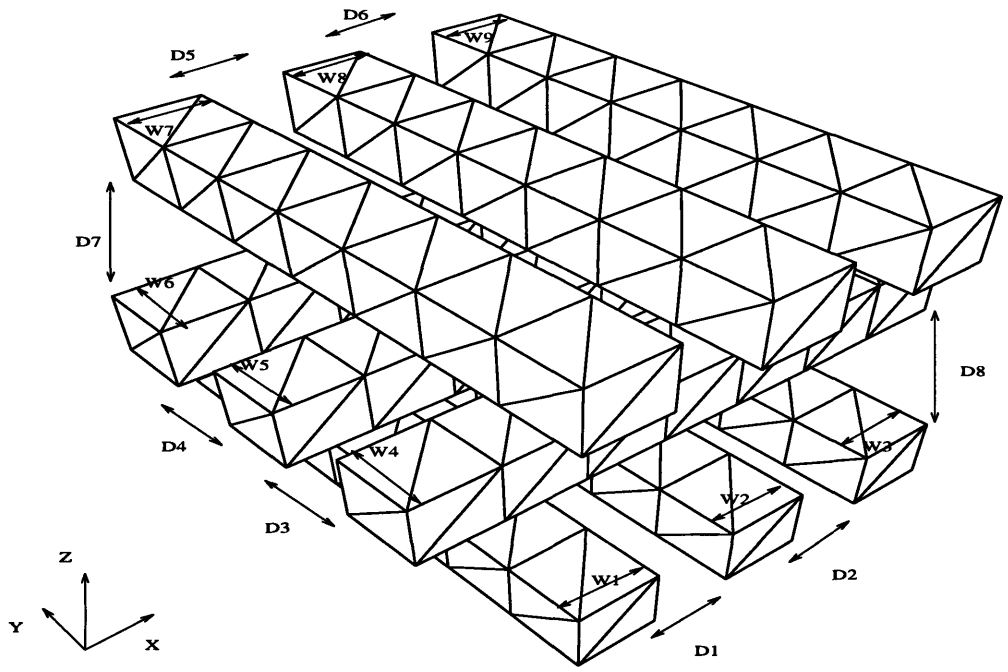

Figure 4-2: Three by three bus structure for capacitance sensitivity analysis

sensitivity computation, and the derivative method can be made even faster by adjoint method. Assume the process variation by d translates into the perturbation vector of $\hat{u}$, then the sensitivity of C_{55} can be written as:

$$\frac{\partial C_{55}}{\partial d} = S_5^T \frac{\partial q_5}{\partial d} \tag{4.7}$$

$$P\frac{\partial q_5}{\partial d} = -\frac{\partial \bar{P}}{\partial u}\hat{u} \tag{4.8}$$

which is equivalent to:

$$\frac{\partial C_{55}}{\partial d} = S_5^T P^{-1}(\frac{\partial \bar{P}}{\partial u}\hat{u}) \tag{4.9}$$

Denote Y as the transpose of $S_5^T P^{-1}$, then Y just needs to be solved once by:

$$P^T Y = S_5$$

This can be solved by one setup of Precorrected FFT for potential evaluation and a GMRES solve of the linear system. For this case, however, Y is also well approximated by q_5 because P is almost symmetric.

With Y resolved, the sensitivity is just:

$$\frac{\partial C_{55}}{\partial d} = q_5^T(\frac{\partial P}{\partial u}\hat{u})$$

where $\frac{\partial \bar{P}}{\partial u}\hat{u}$ is the electrostatic geometric sensitivity to the perturbation of $\hat{u}$.

For the 17 process variations, the total time for sensitivity computation is:

$$t_{der} \approx t_s + t_e \times 17 = 22.005872 + 0.153232 \times 17 \approx 24.61 \; sec$$

where $t_s = 22.005872 \; sec$ is the overall time of setup stage, including one setup of the Precorrected FFT method for potential evaluation, one GMRES solve for q_5 and one setup of the Precorrected FFT method for electrostatic geometric sensitivity computation; $t_e = 0.153232 \; sec$ is the evaluation time for any perturbation vector, which is mostly that of the evaluation stage of the fast algorithm of electrostatic geometric sensitivity computation.

For this example, the derivative method based on the fast algorithm of electrostatic geometric sensitivity computation is more than three times faster than the finite difference method.

Two examples of the result of the computation is, $\frac{\partial C_{55}}{\partial d_1} = -0.012$ and $\frac{\partial C_{55}}{\partial d_3} = 0.492$

.

Bibliography

[1] Narayon R. Aluru and Jacob K. White. Direct-newton finite-element/boundary-element technique for micro-electromechanical analysis. In *Technical Digest IEEE Solid-State Sensor and Actuator Workshop*, Hilton Head Island, SC, June 1996.

[2] J. Funk M. Bachtold, J. Korvink and H. Baltes. New convergence scheme for self-consistent electromechanical analysis of imems. In *Proceedings of International Electronic Devices Meeting*, 1995.

[3] Keith Nabors and Jacob White. Fastcap: A multipole accelerated 3-d capacitance extraction program. *IEEE Transactions on Computer-Aided Design*, 10(11):1447–1459, November 1991. This is a full ARTICLE entry.

[4] J.N. Newman. Distributions of sources and normal dipoles over a quadrilateral panel. *Journals of Engineering Mathematics*, pages 113–126, 1986.

[5] J. Phillips and J. White. A precorrected-FFT method for capacitance extraction of complicated 3-D structures. In *Proceedings of the Int. Conf. on Computer-Aided Design*, November 1994.